Dramatic consequences of reducing erythrocyte membrane cholesterol on *Plasmodium falciparum*

Avantika I. Ahiya[a], Suyash Bhatnagar[a], Joanne Morrisey[a], Josh R. Beck[b], Akhil B. Vaidya[a*]

a. *Center for Molecular Parasitology, Institute for Molecular Medicine and Infectious Disease, Department of Microbiology and Immunology, Drexel University College of Medicine, Philadelphia, Pennsylvania 19129*

b. *Department of Biomedical Sciences, Iowa State University, Ames, Iowa 50011*

*To whom correspondence should be addressed at Center for Molecular Parasitology, Dept. of Microbiology and Immunology, Drexel University College of Medicine, 2900 Queen Lane, Philadelphia, PA 19129. Tel.: 215-991- 8557; Fax: 215-848-2271;

E-mail: av27@drexel.edu

Abstract

Cholesterol is the most abundant lipid in the erythrocyte. During its blood stage development, the malaria parasite establishes an active cholesterol gradient across the various membrane systems within the infected erythrocyte. Interestingly, some antimalarial compounds have recently been shown to disrupt cholesterol homeostasis in intraerythrocytic stages of *Plasmodium falciparum*. These studies point to the importance of cholesterol for parasite growth. Previously, reduction of cholesterol from the erythrocyte membrane by treatment with methyl-ß-cyclodextrin (MßCD) was shown to inhibit parasite invasion and growth. In addition, MßCD treatment of trophozoite stage *P. falciparum* was shown to result in parasite expulsion from the host cell. We have revisited these phenomena by using live video microscopy, ultrastructural analysis, and response to antimalarial compounds. By using time-lapse video microscopy of fluorescently tagged parasites, we show that MßCD treatment for just 30 min causes dramatic expulsion of the trophozoite stage parasites. This forceful expulsion occurs within 10 sec. Remarkably, the plasma membrane of the host cell from which the parasite has been expelled does not appear to be compromised. The parasitophorous vacuolar membrane (PVM) continued to surround the extruded parasite, but the PVM appeared damaged. Treatment with antimalarial compounds targeting PfATP4 or PfNCR1 prevented MßCD-mediated extrusion of the parasites, pointing to a potential role of cholesterol dynamics underlying the expulsion phenomena. We also confirmed the essential role of erythrocyte plasma membrane cholesterol for invasion and growth of *P. falciparum*. This defect can be partially complemented by cholesterol and desmosterol but not with epicholesterol, revealing stereospecificity underlying cholesterol function. Overall, our studies advance previous observations and reveal unusual cell biological features underlying cholesterol depletion of infected erythrocyte plasma membrane.

Keywords:

Malaria, *Plasmodium falciparum*, parasite extrusion, cholesterol dynamics, PfATP4 and PfNCR1 inhibitors, vomocytosis

42 **Importance:**
43
44 Malaria remains a major challenge in much of the world. Symptoms of malaria are caused by the
45 growth of parasites belonging to *Plasmodium* spp. inside the red blood cells (RBC), leading to their
46 destruction. The parasite depends upon its host for much of its nutritional need. Cholesterol is a
47 major lipid in the RBC plasma membrane, which is the only source of this lipid for malarial parasites.
48 We have previously shown that certain new antimalarial compounds disrupt cholesterol homeostasis
49 in *P. falciparum*. Here we use live time-lapse video microscopy to show dramatic expulsion of the
50 parasite from the host RBC when the cholesterol content of the RBC is reduced. Remarkably, this
51 expulsion is inhibited by the antimalarials that disrupt lipid homeostasis. We also show
52 stereospecificity of cholesterol in supporting parasite growth inside RBC. Overall, these results point
53 to a critical role of cholesterol in physiology of malaria parasites.
54

55 **Introduction:**

56 A salient feature of malaria parasites is their dependence on the host to fulfil their nutrient
57 requirements. In addition to various nutrients, *Plasmodium* salvages lipids and fatty acids from the
58 host. While the parasite possesses pathways for synthesizing and modifying lipids (1, 2), it lacks the
59 machinery for *de novo* cholesterol synthesis (3-6). Unlike the intrahepatic stages where the parasites
60 have access to copious amounts of cholesterol (7), blood stage parasites can only access cholesterol
61 present in the erythrocyte membrane (8). Recent studies from our laboratory have identified
62 antimalarials that inhibit two parasite plasma membrane (PPM) transporters, PfATP4 and PfNCR1,
63 which disrupt cholesterol and lipid homeostasis in the PPM (9, 10). Upon treatment with these
64 compounds, there is a rapid accumulation of cholesterol in the PPM rendering the parasites sensitive
65 to the cholesterol dependent detergent saponin. This was observed as the loss of cytosolic proteins in
66 drug treated parasites exposed to saponin. This effect was reversible indicating an active mechanism
67 of cholesterol dynamics within the parasite (9). These unexpected consequences of exposure to novel
68 antimalarials suggest the presence of mechanisms that influence cholesterol transport within
69 intraerythrocytic *P. falciparum*. Previously, it was shown that intra-erythrocytic *P. falciparum* growth
70 requires a supply of fatty acids that cannot be substituted with lipids and cholesterol from serum
71 derived lipoproteins (11). Furthermore, studies from the Haldar laboratory have shown that
72 cholesterol in the erythrocyte plasma membrane is essential for invasion and growth of *P. falciparum*.
73 Interestingly, reduction of cholesterol from the erythrocyte plasma membrane by treatment with
74 MßCD resulted in extrusion of the trophozoite stage parasites (12).

75 Given the observations regarding effects of new antimalarials on cholesterol dynamics and
76 the consequences of cholesterol reduction from infected erythrocyte plasma membrane, we wished to
77 examine a potential link between these phenomena. We have used live fluorescence video
78 microscopy, transmission electron microscopy and treatment with antimalarials to revisit previous
79 findings regarding the consequences of MßCD treatment of intra erythrocytic *P. falciparum*. Results
80 from our experiments confirm and extend these observations and raise important mechanistic
81 questions regarding the role of cholesterol in *P. falciparum* biology.

82

83 **Results:**

84

85 ***Dramatic expulsion of trophozoite stage parasites upon treatment with*** MβCD

86 A previous study showed that treatment of trophozoite stage parasites with MβCD releases
87 the parasites from the erythrocyte. In this study, the authors used filipin and ethidium bromide
88 staining of glutaraldehyde-fixed parasites and did not assess disposition of PVM and PPM in extruded
89 parasites (13). We aimed to examine this effect in real-time using time lapse video microscopy as well
90 as to assess the disposition of PVM and PPM. For this purpose, we used two different transgenic *P.*
91 *falciparum* lines: in one line, the gene encoding PPM-localized PfVP1 was tagged with mNeonGreen
92 at its endogenous locus [kindly provided by Dr. Hangjun Ke; (14)] . The second line expressed two
93 different fluorescently tagged proteins generated by using the CRISPR/Cas9 approach as described in
94 Fig. 1 A and B. The gene encoding PVM-localized EXP2 was tagged with mRuby3 at its endogenous
95 location, and the gene encoding the RhopH complex protein RhopH2 was tagged with mNeonGreen
96 (Fig. 1 A and B). As shown in Fig. 1C, tagging these proteins with fluorescent markers did not affect
97 their proper expression and localizations. EXP2 was expressed all stages and localized to the PVM,
98 whereas RhopH2 was expressed at the highest level in mature stages of the parasite and localized to
99 the punctate rhoptries in the schizont stage. RhopH2 is initially stored in merozoite rhoptries and
100 secreted into the parasitophorous vacuole (PV) during invasion, eventually trafficking to the host cell
101 membrane (15), as seen in ring stages (Fig. 1C) . The use of these parasite lines permitted us to
102 monitor the PPM, PVM and rhoptries of the parasite when exposed to MßCD using live fluorescent
103 microscopy. The trophozoites and early schizont stage-infected erythrocytes were attached to poly-L-
104 lysine coated plates, stained with fluorescent probes for the RBC membrane and nuclei followed by
105 treatment with MßCD for 30 mins. MßCD was removed by washing with the culture medium and the
106 parasites were observed by live time-lapse fluorescent video microscopy. As shown in Fig. 2A and
107 Supplementary Video 1, the parasite extruded out of the host erythrocyte in a dramatic fashion. This
108 expulsion occurred 10-15 min after MβCD was washed off, but the transition from being intracellular
109 to being extracellular occurred in less than 10 seconds. The extruded parasites were surrounded by

110 PPM (in green, Fig. 2B) as well as the PVM (in red, Fig. 2C; Supplementary Fig. 1). Depending upon
111 the plane from which the parasite emerges from the erythrocyte, parts of the PVM were observed still
112 tethered to the host cell. In contrast to the late stage parasites, cholesterol depletion of ring stage
113 parasites did not result in extrusion; RhopH2 was partially localized to the erythrocyte plasma
114 membrane in the ring stage parasites, but the parasite remained inside the host cell (Fig. 2D,
115 Supplementary video 3). Quantification of this phenomenon showed that about 70% of the late stage
116 parasites extruded upon MßCD treatment (Fig. 2E).

117 The exclusion phenomenon was also observed by phase contrast microscopy of the infected
118 erythrocytes treated with 5mM MßCD, which also showed that the late stages extrude out of the
119 erythrocyte without causing lysis of the erythrocytes (Supplementary Fig. 2). We assessed integrity
120 of the erythrocyte membrane by staining MβCD treated cultures with fluorescent phalloidin.
121 Phalloidin stains F-actin underlying the erythrocyte membrane when able to enter the cell. Parasite
122 cultures not exposed to MβCD showed minimal phalloidin staining of either infected or uninfected
123 erythrocytes. On the other hand, 60-70% of both uninfected and infected erythrocyte cytoskeletons
124 were stained with phalloidin in MβCD-treated culture (Supplementary Fig. 3). These observations
125 suggest that MβCD causes a breach in the erythrocyte membrane in a manner that allows phalloidin to
126 enter the cell but without causing catastrophic lysis that would release most of its cytosolic content.
127 This breach in erythrocyte membrane was seen in ring stage infected cells as well, yet this did not
128 result in their expulsion.

129 The forceful expulsion of the parasite from the host cell remains mechanistically unexplained.
130 MßCD treatment of mammalian cells has been shown to affect actin polymerization (16). Thus, one
131 possibility could be that rearrangement and polymerization of RBC cytoskeletal actin may underlie
132 the parasite extrusion. To test this, we treated trophozoite-infected erythrocytes with the actin
133 polymerization inhibitor, Cytochalasin D (CytD) (17). Treatment with CytD prior to MßCD treatment
134 did not inhibit MßCD mediated extrusion of the parasites. Treatment with CytD alone did not cause
135 the parasites to extrude out; however, we did observe defects in the PVM of the CytD treated parasites

136 (Fig. 2F, Supplementary video 2). Although CytD did affect the morphology of the PVM, it failed to
137 prevent extrusion of the parasites when exposed to MßCD.
138 To assess the disposition of membranes of extruded parasites in some detail, we performed
139 transmission electron microscopy of mature stage parasites treated with MßCD. The extruded
140 parasites were still surrounded by PVM, but the PVM was compromised at multiple places (Fig. 2G).
141 The PPM on the other hand remained intact with minimal changes in the intracellular structures.
142 Images shown here are representative of multiple electron micrographs.
143
144 ***Prior Treatment with novel antimalarials abrogates MßCD mediated parasite extrusion***
145 We have previously shown that inhibition of PPM transporters, PfATP4 or PfNCR1 alter
146 cholesterol dynamics in the PPM of late stage parasites (9, 10, 18). We therefore examined the
147 effects of these cholesterol homeostasis disruptors on MßCD-mediated extrusion phenomenon. We
148 treated late stage parasites for 2 hours with KAE609 (a PfATP4 inhibitor), MMV009108 (a PfNCR1
149 inhibitor) or chloroquine (a heme detoxification inhibitor) followed by cholesterol depletion with
150 MßCD. Interestingly, the parasite extrusion was greatly reduced by prior exposure to PfATP4 and
151 PfNCR1 inhibitors but not by chloroquine (Fig. 3A). Quantitation of this phenomenon showed that
152 80% of parasites treated with DMSO or chloroquine extruded following MßCD treatment, whereas
153 only about 25% did so following treatment with PfATP4 and PfNCR1 inhibitors (Fig. 3B). This
154 quantitation was also supported by observation of intracellular and extracellular parasites in Giemsa-
155 stained thin blood smear (Fig. 3C and D). These results suggest that disruption of normal cholesterol
156 dynamics in mature stage parasite results in inhibition of MßCD mediated extrusion of parasites.
157
158 ***Role of erythrocyte plasma membrane cholesterol in invasion and the intra-erythrocytic***
159 ***development of P. falciparum***
160 Previous studies have shown that reduction of erythrocyte plasma membrane cholesterol by
161 treatment with MßCD resulted in inhibition of parasite growth (12). Since we found that the ring stage
162 parasites were not extruded from the erythrocyte by MßCD treatment, we went on to examine the
163 effects of MßCD treatment of ring stage parasites for their intra-erythrocytic developmental cycle

164 (IDC). In addition, we also examined the consequence of complementing cholesterol depleted ring
165 stage parasites with different sterols such as cholesterol, desmosterol or epicholesterol (structures
166 shown in Fig. 4A). We treated the ring stage infected erythrocytes with MßCD for 30 mins followed
167 by washes with normal culture medium. Development of ring stage parasites was assessed by
168 examination of Giemsa-stained thin smears. As shown in Fig. 4B, parasites in the control cells
169 proceeded normally through the IDC and formed trophozoites and rings. In contrast, ring stage
170 parasites growing in cholesterol depleted erythrocytes (MßCD treated) progressed to form what
171 appeared to be trophozoites but failed to mature. Reconstitution with MßCD saturated with
172 cholesterol (CD/Cho) or desmosterol (CD/Des) appeared to restore normal IDC progression. On the
173 other hand, reconstitution with epicholesterol (CD/Epi) did not restore normal IDC, suggesting the
174 importance of stereospecificity of cholesterol polar moiety in supporting parasite development. We
175 also attempted to reconstitute with lanosterol or ß-sitosterol but could not assess it since these resulted
176 in lysis of erythrocytes. To assess the viability of the ring stage parasites growing in MßCD-treated or
177 sterol-reconstituted erythrocytes, we split the culture 1:10 into untreated normal erythrocytes. This
178 was followed by measuring parasitemia over a subsequent four-day period. As shown in Fig 4C, ring
179 stage parasites growing in cholesterol-depleted or epicholesterol-reconstituted cells failed to
180 propagate over the next two cycles. On the other hand, cholesterol- or desmosterol-reconstituted ring
181 stage parasites were able to propagate at a level of about 50% compared to the control ring stage
182 parasites. To assess progression of ring stage parasites, we measured hypoxanthine incorporation
183 over a 24-hour period. As shown in Fig 4D, there was significant reduction in hypoxanthine
184 incorporation in MßCD treated and epicholesterol reconstituted parasites, whereas ring stage parasites
185 in cholesterol or desmosterol reconstituted cells were able to incorporate hypoxanthine.
186 We examined the parasites by transmission electron microscopy at 24 and 48 hours in control
187 and following MßCD treatment. As expected at 24 hours the trophozoites in the control group
188 displayed normal morphology with distinctive internal structures and normal hemozoin formation and
189 went on to form ring stages at 48 hours (Fig 4E, top panel; Supplementary Fig. 1). In contrast MßCD
190 treated ring stages showed abnormal morphology with diminished food vacuoles at 24 hours. These
191 parasites failed to develop into normal schizonts and did not egress at 48 hours after MßCD treatment.

192 (Fig 4E, lower panel; Supplementary Fig 4). These results suggest a defect in normal trophozoite
193 development in erythrocytes with depleted cholesterol content.
194 We also assessed the ability of merozoites to invade and establish infection in MßCD treated
195 erythrocytes. MßCD treated erythrocytes were added to Percoll enriched schizonts. As shown in Fig
196 5A, reduced cholesterol content in uninfected erythrocytes prevented merozoite invasion. The
197 merozoites appeared to remain attached to the surface of MßCD treated erythrocytes but failed to
198 penetrate. Importantly, reconstitution of MßCD treated RBCs with cholesterol complemented this
199 invasion defect (Fig. 5B). Furthermore, the parasites were able to grow in these reconstituted
200 erythrocytes and undergo normal IDC progression. Splitting the cultures 1:10 with addition of normal
201 erythrocytes resulted in continued normal IDC progression of parasites from control and cholesterol
202 reconstituted cells but not from cholesterol deficient cells (Fig. 5C).
203 Different *P. falciparum* strains invade using different pathways: a sialic acid dependent or a
204 sialic acid independent pathway (19, 20). To see if cholesterol in the erythrocyte membrane is
205 selective for a given pathway, we added schizonts of either NF54 (sialic acid dependent) or Dd2
206 (sialic acid independent) strains to MßCD treated erythrocytes. Merozoites from neither strain were
207 able to invade MßCD treated erythrocytes (Fig. 5D).
208
209
210
211 **Discussion**:
212 Using live video microscopy of fluorescently tagged parasites, we have extended previous
213 observations showing expulsion of trophozoite stage *P. falciparum* upon treatment with MßCD. We
214 also showed that this expulsion is inhibited by new antimalarial compounds that disrupt cholesterol
215 homeostasis in the parasite. The dramatic expulsion of the trophozoite stage parasites following
216 MßCD treatment remains unexplained. It is hard to perceive how an intracellular parasite can escape
217 out of the host erythrocyte without causing catastrophic lysis of the host membrane in response to
218 reduction in the cholesterol content in the erythrocyte plasma membrane. Expulsion of the parasite
219 occurs after 40-45 min exposure to MβCD and after MβCD is washed off. Actual expulsion,

220 however, occurs within seconds. The force with which the expulsion appears to occur suggest an
221 active process mediated either by the host or the parasite. Our observation that Cytochalasin D did not
222 prevent expulsion of trophozoites indicates that actin polymerization is not required for this process.
223 Osmotic pressure build-up through solute uptake in trophozoites resulting in their release from the
224 host cells has been widely used for synchronization of blood stage *P. falciparum*. However, this
225 requires incubation with high (about 0.5 M) concentration of solutes such as sorbitol. At 5 mM
226 concentration, MßCD exposure does not pose an osmotic challenge, and at ~1300 Da molecular
227 weight MßCD would not be taken up by the trophozoite-infected erythrocyte through its new
228 permeability pathway. Furthermore, sorbitol-mediated expulsion of the parasite occurs within a few
229 minutes and is accompanied by catastrophic lysis of the infected erythrocyte. In contrast, expulsion
230 caused by MβCD-mediated cholesterol depletion occurs after 40-45 min when MβCD is no longer
231 present, and the infected erythrocyte does not undergo lysis. Also, the MβCD-mediated expulsion is
232 inhibited by prior treatment with PfATP4 and PfNCR1 inhibitors. These observations seem to argue
233 against an osmotic imbalance as the force underlying the expulsion phenomenon described here. We
234 speculate the possibility of a hitherto unrecognized process through which the parasite might sense
235 cholesterol content of the erythrocyte membrane. It is of interest to note that MßCD-mediated
236 expulsion of the parasite resembles expulsion of fungal pathogens from the mammalian cells through
237 a process termed vomocytosis wherein the expulsion does not result in lysis of the host cell (21-23).
238
239 Inhibition of the parasite expulsion by compounds that inhibit PfATP4 or PfNCR1was
240 unexpected; this inhibition was not a result of parasite demise since chloroquine failed to do so. We
241 have previously shown that both these inhibitors induce cholesterol accumulation in the PPM in a
242 reversible manner (10). PfATP4 inhibition results in Na^+ influx into the parasite and a collapse of Na^+
243 gradient across the PPM. We propose that PfNCR1 requires a Na^+ gradient to maintain cholesterol
244 homeostasis, and its collapse by PfATP4 inhibition results in indirect inhibition of PfNCR1. The net
245 result of both PfATP4 and PfNCR1 inhibition, therefore, is a disruption of cholesterol homeostasis in
246 late-stage *P. falciparum*. We envision a dynamic movement of cholesterol between various

247 membranes of infected erythrocytes. Recent investigations have also supported the notion of
248 cholesterol gradients in infected erythrocytes (24-28). Reduction of the plasma membrane cholesterol
249 content, thus, appears to be sensed by the parasite in a manner that results in the expulsion of
250 trophozoites.

251 The erythrocyte plasma membrane contains large amounts of cholesterol (50 mole% of total
252 lipids). Upon infection by *Plasmodium*, the PVM acquires cholesterol but the PPM remains highly
253 deficient in cholesterol. Indeed, this fact is the basis for widely used saponin mediated freeing of
254 intra-erythrocytic parasites. Previous studies have suggested the importance of cholesterol for *P.*
255 *falciparum* growth and invasion (12, 13, 25). A recent study using lattice light scattering microscopy
256 demonstrated the importance erythrocyte membrane remodeling for the formation of the PVM, a
257 process in which cholesterol is likely to play a significant role [11]. We observed that that ring stage
258 parasites growing in cholesterol deficient erythrocytes fail to fully progress. Furthermore, the
259 digestive vacuoles of trophozoite-like parasites at 24 hours after MßCD treatment of ring stages had
260 unusual morphology (Fig.3E and Supplementary figure 1). At 48 hours after MßCD treatment of ring
261 stages, parasites appeared to attempt segmentation without being able to form mature merozoites (Fig.
262 3E and Supplementary figure 1). One possible explanation could be that cholesterol dynamics assist
263 lipid and/or fatty acid import to sustain parasite growth. The fact that cholesterol and desmosterol (but
264 not epicholesterol) could substantially rescue these defects suggest stereospecificity in the role of
265 cholesterol to sustain parasite growth. Further studies will be required to gain mechanistic insights
266 into cholesterol dynamics and their contribution to parasite growth.
267
268
269 **Methods**:
270 **Parasite lines and culture conditions**

271 Experiments were carried out using different *P. falciparum* tagged lines. 1) the 3D7 strain in
272 which endogenous PfVP1 gene was tagged with mNeon green (mNG) at the C-terminal end
273 (PfVP1-mNG) (14). This line was used for monitoring the dynamics of the parasite plasma

274 membrane; 2) the NF54 strain in which endogenous RhopH2 gene was tagged with mNG and
275 the endogenous Exp2 gene tagged with mRuby3 (NF54 Rhoph2/Exp2). Cloning was carried
276 out with Infusion (Clontech) and NEBuilder HiFi (NEB). To generate an endogenous EXP2-
277 mRuby3 fusion, 5' and 3' homology flanks targeting the 3' end of *exp2* were PCR amplified
278 from plasmid pyPM2GT-EXP2-mNG (29) using primers
279 CACTATAGAACTCGAGGGAGAAACAATCTTTTATATAAAATGTACAGAGTTTGA
280 AAG and
281 TCCTCCACTTCCCCTAGGTTCTTTATTTTCATCTTTTTTTTCATTTTTAAATAAATC
282 TCCAC and inserted between *XhoI* and *AvrII* sites in the plasmid pbPM2GT (30). The
283 mRuby3 coding sequence was then amplified from plasmid pLN-HSP101-SP-mRuby3(31)
284 using primers GATGAAAATAAAGAACCTAGGGGAAGTGGAGGAGTG and
285 TAACTCGACGCGGCCGTCACTTGTACAGCTCGTCCATGCC and inserted between
286 *XhoI* and *AvrII*, resulting in the plasmid pbEXP2-mRuby3. This plasmid was linearized at the
287 *AflII* site between the 3′ and 5′ homology flanks and co-transfected with pUF-Cas9-EXP2-
288 CT-gRNA into NF54^{attB}::HSP101^{DDD} (31) . Parasites were maintained in 10 µM trimethoprim
289 (TMP) to stabilize the HSP101^{DDD} fusion and selection with 2.5 µg/ml Blasticidin S was
290 applied 24 hours post transfection. A clonal line bearing the EXP2-mRuby3 fusion was
291 derived by limiting dilution after parasite returned from selection and designated
292 NF54^{attB}::HSP101^{DDD}+EXP2-mRuby3.

293 For generation of an endogenous RhopH2-mNG fusion, a gRNA target site was chosen
294 upstream of the *rhoph2* stop codon (TCTTCACTGATTTCTTTGTA) and the gRNA seed
295 sequence was synthesized as a sense and anti-sense primer pair (sense shown)
296 TAAGTATATAATATTTCTTCACTGATTTCTTTGTAGTTTTAGAGCTAGAA, annealed
297 and inserted into the *AflII* site of the plasmid pAIO3 (32), resulting in the plasmid pAIO3-
298 RhopH2-CT-gRNA. To integrate mNG at the 3' end of *rhoph2*, a 5' homology flank (up to

299 but not including the stop codon) was amplified from NF54^{attB} genomic DNA using primers
300 AATTTCATCATTATGAAAGTTCTCAGCTTAAGAAGCATATATTAAGAATATAGTT
301 TCAGA and
302 CCTCCACTTCCCCTAGGACTGCTCTTCAGAATATACAGGTTTTTTATAAGATCCTC
303 CGATATCTCCTTATATGGATCAGATATATCTGAGAAA, incorporating several
304 synonymous mutations in the seed sequence of the gRNA target site within the *rhoph2*
305 coding sequence. A 3' homology flank (beginning at the endogenous stop codon) was
306 amplified using primers
307 GTGACACTATAGAACTCGAGTAAACGTTAAAAAAAAAATATATATAAGGAGAAA
308 GCACTG and
309 TCTGAAACTATATTCTTAATATATGCTTCTTAAGCTGAGAACTTTCATAATGATGA
310 AATT, assembled in a second PCR reaction using primers
311 GTGACACTATAGAACTCGAGTAAACGTTAAAAAAAAAATATATATAAGGAGAAA
312 GCACTG and
313 CCTCCACTTCCCCTAGGACTGCTCTTCAGAATATACAGGTTTTTTATAAGATCCTC
314 CGATATCTCCTTATATGGATCAGATATATCTGAGAAA and inserted between *XhoI*
315 and *AvrII* sites in pyPM2GT-EXP2-mNG (29) resulting in the plasmid pyPM2GT-RhopH2-
316 mNG. This plasmid was linearized at the *AflII* site between the 3' and 5' homology flanks
317 and co-transfected with pAIO3-RhopH2-CT-gRNA into NF54^{attB}::HSP101^{DDD}+EXP2-
318 mRuby3. Selection with 2 µM DSM-1 was applied 24 hours post transfection (along with 10
319 µM trimethoprim). After parasites returned from selection, a clonal line containing the EXP2-
320 mRuby3 and RhopH2-mNG fusions was obtained by limiting dilution and designated
321 NF54^{attB}::HSP101^{DDD}+EXP2-mRuby3+RhopH2-mNG. Correct integration of the transgenes
322 was confirmed by PCR amplifications using the following primers (indicated in Fig. 1):
323 A:CCAGAATGTTTCGGACCATGTAC; B: TGGTATCCGGAGCCATCTACCATG; C:

324 CACTTTGTAACTTCATTTTCTAAAATGACCTTGTTC; D: GCAACAAGTGCCTTAACCACCG; E:
325 CGATGACTTTGATCCTCATGGTTTGC; and F: TCACTTATGTTGTATAGAGACACAATTCGT

326 This line was used for monitoring the parasitophorous vacuolar membrane and to mark the
327 parasite. *P. falciparum* parasites were cultured in O^+ human blood from Interstate Blood
328 Bank, TN in RPMI 1640 supplemented with 2g/L sodium bicarbonate, 10mg/L
329 hypoxanthine, 15mM HEPES, 50mg/L gentamycin sulphate, 0.5% AlbuMax II. Parasite
330 culture was maintained at 2.5% hematocrit at 37 °C in 90% N_2, 5% CO_2, 5% O_2.

331

332 **Preparation of MßCD and MßCD-sterol complexes**

333 Parasites were treated with 5mM MßCD diluted in appropriate medium from a stock solution
334 of 25mM MßCD (Catalog no. AC377110250) in PBS in appropriate medium. Sterols
335 [Cholesterol (Sigma, C3045-25G) , Desmosterol (Steraloids, catalog no. C3150-000),
336 Epicholesterol (Steraloids, catalog no. C6730-000)] were loaded onto MßCD according to
337 previously published protocol (33). Briefly, 10 µL of 15mg/ml sterols dissolved in ethanol
338 were added to 500 µL 5% w/v MßCD, heated for 10 mins at 80°C and mixed by inverting
339 several times until the solution was clear. The above step was repeated 4 times to add a total
340 of 50µL sterol stock solution. The solution was heated until the sterols were stably
341 incorporated in MßCD (clear solution). MßCD/sterol complexes were snap frozen in dry ice
342 for 2 mins. Subsequently, the MßCD/sterol complexes were lyophilized in a speed vac until
343 all liquid had evaporated and a fluffy powered remained at the bottom of the tube and stored
344 at -20°C. Immediately before use, 375µl of medium was added to the MßCD/sterol
345 complexes and vortexed until dissolved. The MßCD/sterol complexes were sterilized using
346 0.22µm syringe filter.

347

348 **Treatment of parasitized erythrocytes with MBCD and reconstitution with**
349 **MBCD/sterol complexes**
350 Parasite cultures were synchronized by treatment with 0.5M alanine for 10 minutes.
351 Erythrocyte infected with ring stage parasites were treated with 5mM MßCD for 30 mins at
352 37 °C and washed 3 times with pre-warmed RPMI1640 media. Hematocrit was maintained at
353 2.5% throughout the culture and washing steps. The parasites were returned to normal culture
354 conditions. In experiments involving reconstitution with MßCD/sterol complexes, parasites
355 were first treated with MßCD as described above. Following this, the cells were incubated
356 with 1:7 dilution of MßCD/sterol complexes for 30 mins. Parasites were washed 3 times and
357 returned to normal culture conditions. Giemsa-stained thin blood smears were prepared 24
358 and 48 hours after the treatment with MßCD or after reconstitution with MßCD/sterol
359 complexes. The culture at 48 hours was split 1:10 in normal erythrocytes. Growth of the
360 parasites in these cultures were followed for 4 days by examining Giemsa stained thin blood
361 smears
362
363 **Hypoxanthine incorporation of ring stage erythrocyte treated with MßCD or**
364 **MßCD/sterol complexes**
365 Ring stage erythrocyte (1.5% parasitemia) were treated with MßCD for 30 mins and washed
366 3 times with normal medium. The hematocrit was maintained at 2.5%. MßCD-treated ring
367 stage erythrocytes were then treated with either MßCD/cholesterol, MßCD/desmosterol or
368 MßCD/epicholesterol for 30 mins and washed 3 times with low hypoxanthine medium. The
369 hematocrit was then adjusted to 1.5% by addition of low hypoxanthine medium to the cells.
370 200µl of cells were then plated in triplicates in a 96-well plate. Each well was pulsed with 22
371 µl of 0.5 µCi/ml ^{3}H-hypoxanthine (PerkinElmer NET 177) and incubated for 24 hours at
372 37ºC in 5% CO_2, 5% O_2, 90% N_2 chamber. Parasites were lysed by freeze/thaw and were

373 collected on filters using a cell harvester (PerkinElmer LifeSciences). This was followed by
374 addition of MicroScint O scintillation cocktail and incorporation of ^{3}H-hypoxanthine was
375 measured using a TopCount scintillation counter (PerkinElmer Life-sciences).
376
377 **Parasite invasion in MßCD or MßCD/Cholesterol treated erythrocytes**
378 We treated 500 µl of 50% hematocrit erythrocytes with 5mM MßCD for 30 mins followed by
379 3 washes. In addition, similarly treated erythrocytes were reconstituted with
380 MßCD/Cholesterol for 30 mins followed by 3 washes. Synchronized late stages trophozoites
381 were enriched by centrifugation over a 70% Percoll cushion (3000 RPM, 20 mins) and
382 washed thrice with medium. Enriched late stage trophozoites were added to MßCD-treated,
383 MßCD/Cholesterol-reconstituted and control erythrocytes. Giemsa-stained thin blood smears
384 were prepared 24 and 48 hours following the addition. The culture at 48 hours was split 1:10
385 in normal erythrocytes. Growth of the parasites in these cultures were followed for 4 days by
386 examining Giemsa-stained thin blood smears.
387
388
389 **Live microscopy of parasites**
390 Glass bottom culture dishes (35 mm) were coated with 0.1% poly-L-lysine overnight and
391 washed 3 times with PBS. Parasite culture (250µl at 2.5% hematocrit) was added to the
392 dishes and incubated for 30 mins to allow attachment. Culture dishes were washed 3 times
393 with PBS followed by addition of medium. For MßCD extrusion experiments with NF54
394 Rhoph2/Exp2 line, all washes, incubation and imaging was done in medium supplemented
395 with TMP. Parasites were attached to poly-L-lysine coated plates and incubated in RPMI
396 containing wheat germ agglutinin-Alexa 350 (WGA-350) (Invitrogen, Catalog no. W7024) at
397 5µg/ml final concentration and incubated for 12 mins to stain the erythrocyte plasma

398 membrane. In addition to WGA staining, PfVP1-mNG line was also stained with SYTO deep
399 red nuclear stain for 30 min. Parasites were treated with 5mM MßCD followed by three
400 washes with medium. The medium was replaced with phenol red free medium followed by
401 live fluorescent microscopy. Imaging was done using the Nikon Ti microscope. WGA-Alexa-
402 350 was visualized using DAPI filter set, mNeon green with FITC, SYTO deep red nuclear
403 stain with Cy5 and mRuby was visualized using TRITC filter set. Video microscopy
404 parameters are given in the legends of Supplementary Videos.
405
406 **Inhibition of MßCD mediated extrusion by novel antimalarials**.
407 To look at the effects of antimalarials on MßCD mediated extrusion, parasites were stained
408 with WGA-350 and SYTO deep red for PfVP-1mNG line or WGA-350 for NF54
409 Rhoph2/Exp2 line as described above and treated with 10xEC_{50} concentrations of
410 Choloroquine (150nM), KAE609 (10nM) or MMV009108(1µM) for 2.5 hours prior to 30
411 mins treatment with MßCD and washed thrice with medium. Medium supplemented with
412 drugs (at the concentration mentioned above) was added back to the dish and live fluorescent
413 imaging was carried out. Quantification of parasites remaining inside/outside of erythrocytes
414 was carried out by examining at least 100 different images of individual parasites for each
415 experimental condition.
416 **Cytochalasin D (Cyt-D) treatment prior to MßCD treatment of parasites**
417 Attached NF54 RhopH2/Exp2 trophozoites were stained with WGA-350 for 12 mins,
418 followed by three washes. The cells were then treated with 0.5µM Cyt-D for 45 mins. This
419 was followed by the addition of 5mM MßCD for 30 mins. The culture dishes were washed 3
420 times and live fluorescent microscopy was performed to examine parasite extrusion. In the
421 control condition, parasites were treated with Cyt-D without MßCD treatment.
422

423 **Transmission electron microscopy of trophozoite infected MßCD treated erythrocytes**

424 Erythrocytes infected with trophozoite stage parasites were treated with 5mM **MßCD** for 30
425 mins at 2.5% hematocrit followed by three washes with PBS and incubated in complete
426 medium for 30 mins at 37 °C. Cells were washed once in PBS by gentle centrifugation and
427 fixed with 2% paraformaldehyde, 2.5% glutaraldehyde in 100 mM cacodylate buffer and
428 were fixed for 1 hour at room temperature. Cells were gently pelleted by centrifugation,
429 resuspended in cacodylate buffer and immediately stored on dry ice for shipment.
430 Ring stage infected erythrocytes were treated with 5mM for 30 mins, washed thrice with
431 PBS and returned to culture at 37 °C. At 24 and 48 hours after the treatment, infected
432 erythrocytes were fixed and prepared for transmission electron microscopy as described
433 above.

434 **Phalloidin staining of MßCD treated cultures**

435 Infected erythrocyte cultures from the PfVP1-mNG line were treated with 5mM MßCD for
436 30 mins at 37 °C and washed 3 times with prewarmed RPMI media. Phalloidin staining was
437 carried out as described (34). Briefly, the MßCD treated cultures were stained with
438 Phalloidin Alexa 594 (Invitrogen; diluted 1:50 from a 200 unit ml^{-1} stock in methanol) for 5
439 mins at 37 °C, washed thrice with prewarmed phenol red free RPMI1640. The cells were
440 added to the glass slides and sealed with greased coverslips. Images were taken using the
441 Nikon Ti microscope. mNeongreen was visualized using the FITC channel, Phalloidin Alexa
442 594 was visualized using the TRITC filter set.

443

444

445

446

447 **Acknowledgements:**

448 We thank the members of the Vaidya lab for lively discussion and input. We thank Dr.

449 Hangjun Ke for providing PfVP1-mNG parasite line. This work was supported by a National

450 Institutes of Health grant R01 AI132508 to ABV and R00 HL133453 to J.R.B.

451 **References:**

452 1. Cassera MB, Gozzo FC, D'Alexandri FL, Merino EF, del Portillo HA, Peres VJ,
453 Almeida IC, Eberlin MN, Wunderlich G, Wiesner J, Jomaa H, Kimura EA, Katzin
454 AM. 2004. The methylerythritol phosphate pathway is functionally active in all
455 intraerythrocytic stages of Plasmodium falciparum. J Biol Chem 279:51749-59.
456 2. Gerold P, Schwarz RT. 2001. Biosynthesis of glycosphingolipids de-novo by the
457 human malaria parasite Plasmodium falciparum. Mol Biochem Parasitol 112:29-37.
458 3. Holz GG, Jr. 1977. Lipids and the malarial parasite. Bull World Health Organ 55:237-
459 48.
460 4. Maguire PA, Sherman IW. 1990. Phospholipid composition, cholesterol content and
461 cholesterol exchange in Plasmodium falciparum-infected red cells. Mol Biochem
462 Parasitol 38:105-12.
463 5. Vial HJ, Ancelin ML, Philippot JR, Thuet MJ. 1990. Biosynthesis and dynamics of
464 lipids in Plasmodium-infected mature mammalian erythrocytes. Blood Cells 16:531-
465 55; discussion 556-61.
466 6. Vial HJ, Philippot JR, Wallach DF. 1984. A reevaluation of the status of cholesterol
467 in erythrocytes infected by Plasmodium knowlesi and P. falciparum. Mol Biochem
468 Parasitol 13:53-65.
469 7. Labaied M, Jayabalasingham B, Bano N, Cha SJ, Sandoval J, Guan G, Coppens I.
470 2011. Plasmodium salvages cholesterol internalized by LDL and synthesized de novo
471 in the liver. Cell Microbiol 13:569-86.
472 8. Grellier P, Rigomier D, Clavey V, Fruchart JC, Schrevel J. 1991. Lipid traffic
473 between high density lipoproteins and Plasmodium falciparum-infected red blood
474 cells. J Cell Biol 112:267-77.
475 9. Das S, Bhatanagar S, Morrisey JM, Daly TM, Burns JM, Jr., Coppens I, Vaidya AB.
476 2016. Na+ Influx Induced by New Antimalarials Causes Rapid Alterations in the
477 Cholesterol Content and Morphology of Plasmodium falciparum. PLoS Pathog
478 12:e1005647.
479 10. Istvan ES, Das S, Bhatnagar S, Beck JR, Owen E, Llinas M, Ganesan SM, Niles JC,
480 Winzeler E, Vaidya AB, Goldberg DE. 2019. Plasmodium Niemann-Pick type C1-
481 related protein is a druggable target required for parasite membrane homeostasis.
482 Elife 8.
483 11. Coppens I, Vielemeyer O. 2005. Insights into unique physiological features of neutral
484 lipids in Apicomplexa: from storage to potential mediation in parasite metabolic
485 activities. Int J Parasitol 35:597-615.
486 12. Samuel BU, Mohandas N, Harrison T, McManus H, Rosse W, Reid M, Haldar K.
487 2001. The role of cholesterol and glycosylphosphatidylinositol-anchored proteins of
488 erythrocyte rafts in regulating raft protein content and malarial infection. J Biol Chem
489 276:29319-29.
490 13. Lauer S, VanWye J, Harrison T, McManus H, Samuel BU, Hiller NL, Mohandas N,
491 Haldar K. 2000. Vacuolar uptake of host components, and a role for cholesterol and
492 sphingomyelin in malarial infection. The EMBO journal 19:3556-3564.

14. Solebo O, Ling L, Zhou J, Fu T-M, Ke H. 2021. Plasmodium falciparum vacuolar pyrophosphatase 1 for ring stage development and its transition to trophozoite. bioRxiv doi:10.1101/2021.10.25.465524:2021.10.25.465524.
15. Ahmad M, Manzella-Lapeira J, Saggu G, Ito D, Brzostowski JA, Desai SA. 2020. Live-Cell FRET Reveals that Malaria Nutrient Channel Proteins CLAG3 and RhopH2 Remain Associated throughout Their Tortuous Trafficking. mBio 11.
16. Guerra FS, Sampaio LdS, Konig S, Bonamino M, Rossi MID, Costa ML, Fernandes P, Mermelstein C. 2016. Membrane cholesterol depletion reduces breast tumor cell migration by a mechanism that involves non-canonical Wnt signaling and IL-10 secretion. Translational Medicine Communications 1:3.
17. Casella JF, Flanagan MD, Lin S. 1981. Cytochalasin D inhibits actin polymerization and induces depolymerization of actin filaments formed during platelet shape change. Nature 293:302-5.
18. Bhatnagar S, Nicklas S, Morrisey JM, Goldberg DE, Vaidya AB. 2019. Diverse Chemical Compounds Target Plasmodium falciparum Plasma Membrane Lipid Homeostasis. ACS infectious diseases 5:550-558.
19. Camus D, Hadley TJ. 1985. A Plasmodium falciparum antigen that binds to host erythrocytes and merozoites. Science 230:553-6.
20. Dolan SA, Miller LH, Wellems TE. 1990. Evidence for a switching mechanism in the invasion of erythrocytes by Plasmodium falciparum. J Clin Invest 86:618-24.
21. Cruz-Acuña M, Pacifici N, Lewis JS. 2019. Vomocytosis: Too Much Booze, Base, or Calcium? mBio 10.
22. Nicola AM, Robertson EJ, Albuquerque P, Derengowski Lda S, Casadevall A. 2011. Nonlytic exocytosis of Cryptococcus neoformans from macrophages occurs in vivo and is influenced by phagosomal pH. mBio 2.
23. Seoane PI, May RC. 2020. Vomocytosis: What we know so far. Cell Microbiol 22:e13145.
24. Fraser M, Jing W, Bröer S, Kurth F, Sander LE, Matuschewski K, Maier AG. 2021. Breakdown in membrane asymmetry regulation leads to monocyte recognition of P. falciparum-infected red blood cells. PLoS Pathog 17:e1009259.
25. Geoghegan ND, Evelyn C, Whitehead LW, Pasternak M, McDonald P, Triglia T, Marapana DS, Kempe D, Thompson JK, Mlodzianoski MJ, Healer J, Biro M, Cowman AF, Rogers KL. 2021. 4D analysis of malaria parasite invasion offers insights into erythrocyte membrane remodeling and parasitophorous vacuole formation. Nat Commun 12:3620.
26. Hayakawa EH, Yamaguchi K, Mori M, Nardone G. 2020. Real-time cholesterol sorting in Plasmodium falciparum-erythrocytes as revealed by 3D label-free imaging. Sci Rep 10:2794.
27. Tokumasu F, Crivat G, Ackerman H, Hwang J, Wellems TE. 2014. Inward cholesterol gradient of the membrane system in P. falciparum-infected erythrocytes involves a dilution effect from parasite-produced lipids. Biol Open 3:529-41.
28. Koch M, Cegla J, Jones B, Lu Y, Mallat Z, Blagborough AM, Angrisano F, Baum J. 2019. The effects of dyslipidaemia and cholesterol modulation on erythrocyte susceptibility to malaria parasite infection. Malar J 18:381.
29. Glushakova S, Busse BL, Garten M, Beck JR, Fairhurst RM, Goldberg DE, Zimmerberg J. 2017. Exploitation of a newly-identified entry pathway into the malaria parasite-infected erythrocyte to inhibit parasite egress. Sci Rep 7:12250.

541 30. Beck JR, Muralidharan V, Oksman A, Goldberg DE. 2014. PTEX component
542 HSP101 mediates export of diverse malaria effectors into host erythrocytes. Nature
543 511:592-5.
544 31. Glushakova S, Beck JR, Garten M, Busse BL, Nasamu AS, Tenkova-Heuser T,
545 Heuser J, Goldberg DE, Zimmerberg J. 2018. Rounding precedes rupture and
546 breakdown of vacuolar membranes minutes before malaria parasite egress from
547 erythrocytes. Cell Microbiol 20:e12868.
548 32. Nessel T, Beck JM, Rayatpisheh S, Jami-Alahmadi Y, Wohlschlegel JA, Goldberg
549 DE, Beck JR. 2020. EXP1 is required for organisation of EXP2 in the
550 intraerythrocytic malaria parasite vacuole. Cell Microbiol 22:e13168.
551 33. Luu W, Gelissen IC, Brown AJ. 2017. Manipulating Cholesterol Status Within Cells.
552 Methods Mol Biol 1583:41-52.
553 34. Collins CR, Hackett F, Atid J, Tan MSY, Blackman MJ. 2017. The Plasmodium
554 falciparum pseudoprotease SERA5 regulates the kinetics and efficiency of malaria
555 parasite egress from host erythrocytes. PLoS Pathog 13:e1006453.
556

557

558

559

560

561 **Figures**

562
563
564
565
566
567
568
569
570

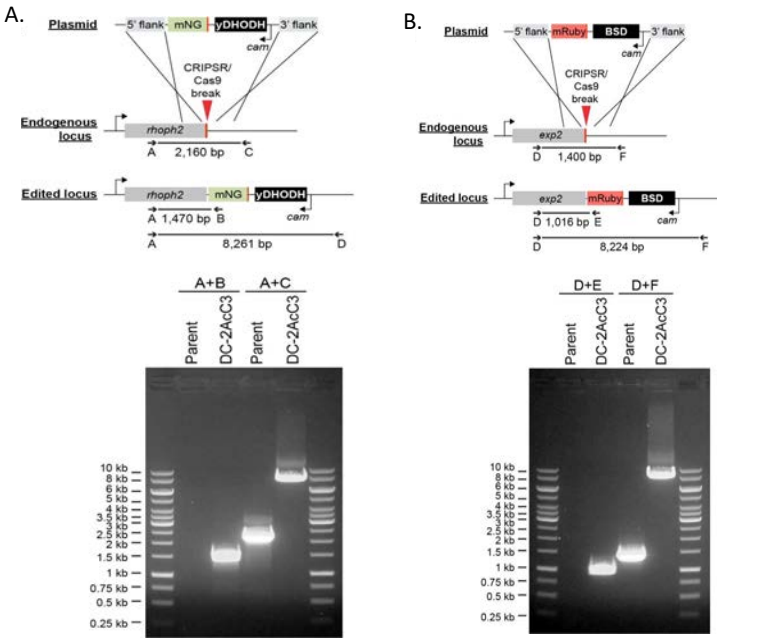

571
572
573
574

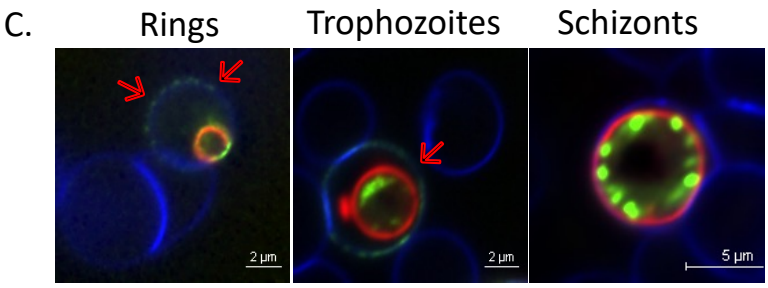

575 **Figure 1:** Generation of the NF54 Rhoph2/EXP2 line : (A) Strategy for tagging *rhoph2* with
576 mNeongreen (mNG) and gel image indicating presence of clonal population expressing
577 *rhoph2-mNG*. (B) Strategy for the tagging *exp2 with mRuby tag* and agarose gel image
578 indicating the presence of clonal population expressing *exp2-mRuby.* Sequences of the
579 diagnostic primers A,B,C, and D are provided in the Materials and Methods. (C) Live
580 fluorescence microscopy images indicating the expected localization of the tagged proteins.
581 Red arrows indicate the dual localization of RhopH2-mNG on the RBC membrane as well as
582 the parasite in the rings and trophozoites while in the schizonts the protein is localized to
583 rhoptries. The EXP2-mRuby marks the PVM of the parasite. Erythrocyte membrane is stained
584 with WGA-Alexa-350 (Blue)

585

586

587

588

589

590

591

592

593

594

595

596

597

598

599

600

601

602

603

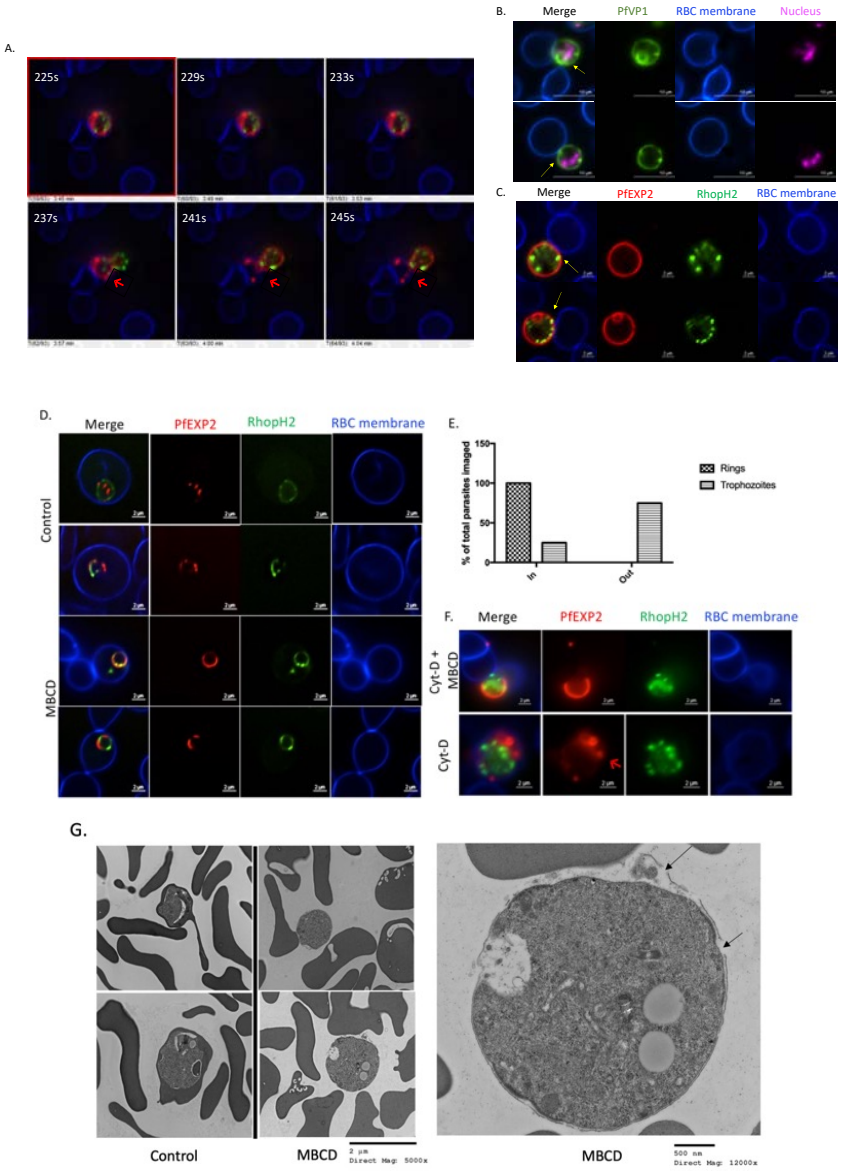

604 **Figure 2:**Trophozoites extrude out from erythrocyte upon treatment with MßCD.

605 (A) Still frames from Supplementary video 1 from time-lapse video microscopy performed at.

606 Parasites extrude out from the erythrocyte with the PVM still tethered to the erythrocyte

607 membrane without causing the lysis of erythrocyte (indicated by arrows). (B) Representative

608 images (>50) of PfVP1- mNG line after MßCD treatment. Nucleus is stained with SYTO-deep

609 red (Pink). (C) Representative images (>50) of NF54 RhopH2/Exp2 line after MßCD

610 treatment. Erythrocyte membrane is stained with WGA-Alexa-350 (Blue). Infected
611 erythrocytes were subjected to live fluorescent microscopy after treatment with MßCD.
612 Parasites extrude out from erythrocyte without causing lysis of the erythrocyte with their PPM
613 (B) and PVM (C) still attached to the erythrocyte as indicated by the arrows. (D) Representative
614 images of erythrocytes infected with ring stages of the NF54 RhopH2/Exp2 line treated with
615 MßCD. Ring stage parasites do not extrude out from erythrocytes. (E) Quantification of
616 parasites remaining inside/outside of erythrocytes after MßCD treatment was carried out by
617 examining at least 100 different images of individual parasites for each experimental condition
618 (100 for ring stages and 330 for trophozoites). (F) Upper panel: Treatment of NF54
619 RhopH2/Exp2 trophozoites with 0.5 µM Cyt-D for 45 mins prior to MßCD treatment does not
620 inhibit parasite extrusion. Lower panel: Treatment with 0.5 µM Cyt-D alone does not cause
621 extrusion of trophozoites but did alter PVM morphology (as indicated by arrows). (G)
622 (Left)Treatment with MßCD causes extrusion of *P. falciparum* stage trophozoites without
623 causing erythrocyte rupture unlike the control group where the trophozoite is still inside the
624 erythrocyte (Scale bar- 2µM, Direct magnification-5,000x). (Right) Zoomed in image of
625 parasite extruded out of erythrocyte after MßCD treatment shows the PVM ruptured at multiple
626 places indicated by black arrows. Electron microscopy of extruded *P. falciparum*. Left panels
627 show lower magnification views of control and MβCD-treated trophozoites. A higher
628 magnification view of an extruded parasite (right panel) shows that the PVM is compromised
629 at multiple places (arrows) (Scale bar-500nM, Direct magnification-12,000x).
630
631

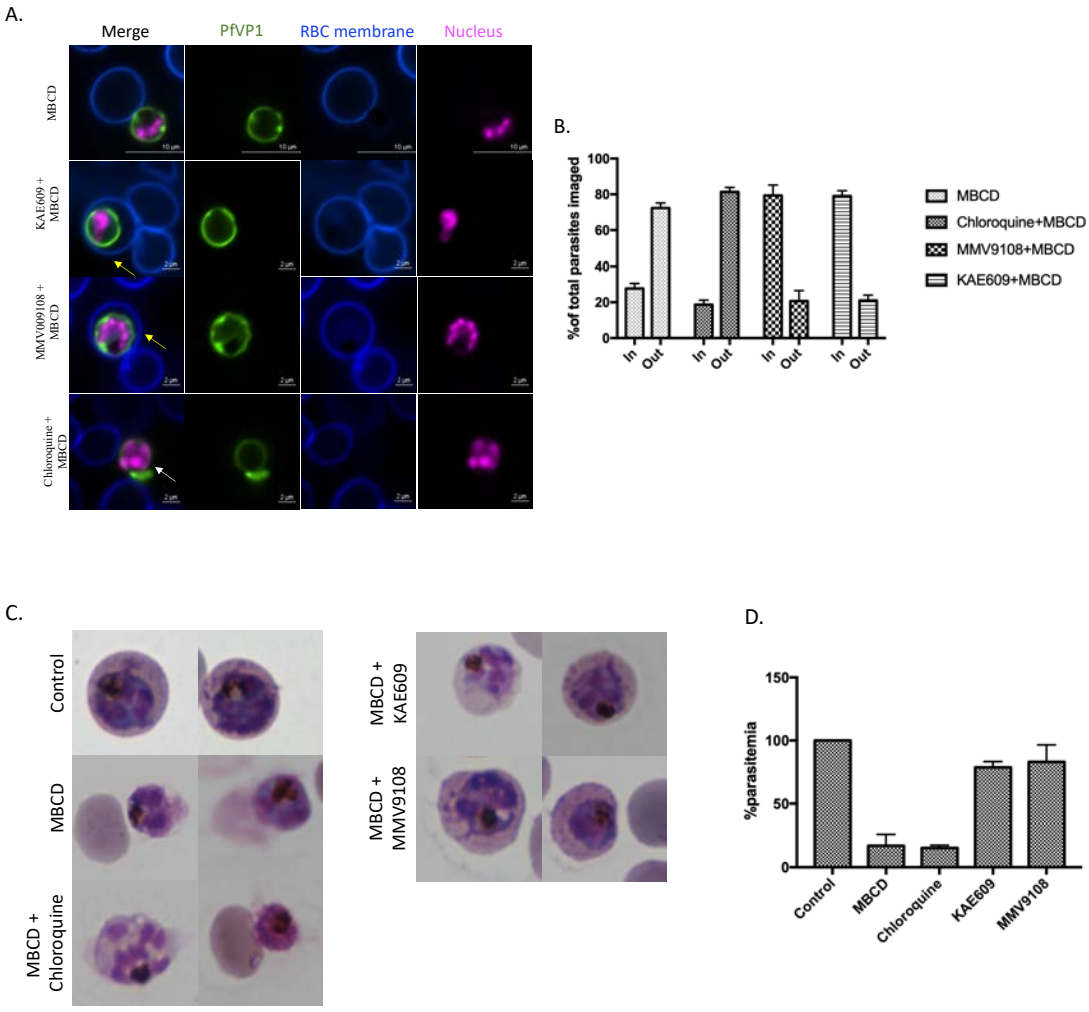

Figure 3 : Treatment with PfATP4 or PfNCR1 inhibitors prior to MßCD treatment inhibited MßCD mediated extrusion of parasites: (A) Trophozoite stage parasites from PfVP1-mNG line were treated with KAE609 (10nM), MMV009108 (1µM) and chloroquine (150nM) prior to treatment with MßCD. Live fluorescent imaging showed that parasite extrusion was inhibited by prior treatment with KAE609 and MMV009108 (indicated by yellow arrows) while treatment with chloroquine like MßCD did not inhibit this extrusion (indicated by white arrows). Nucleus is stained with SYTO-deep red (pink). Erythrocyte membrane is stained with WGA-Alexa-350 (Blue). Representative images from 3 independent experiments for each condition (B) Quantification from live fluorescent microscopy experiments of parasite extrusion upon drug treatment followed by MßCD treatment. Approximately 250 cells for each

657 experimental condition over 4 independent experiment were assessed. (C) Giemsa stained thin
658 blood smears prepared from cultures after treatment with KAE609 (10nM), MMV009108
659 (1μM) and chloroquine (150nM) prior to treatment with MßCD. (D) Quantitation of parasite
660 extrusion upon drug treatment followed by MßCD treatment from Giemsa-stained thin blodd
661 smears (~1000 cells were counted).
662

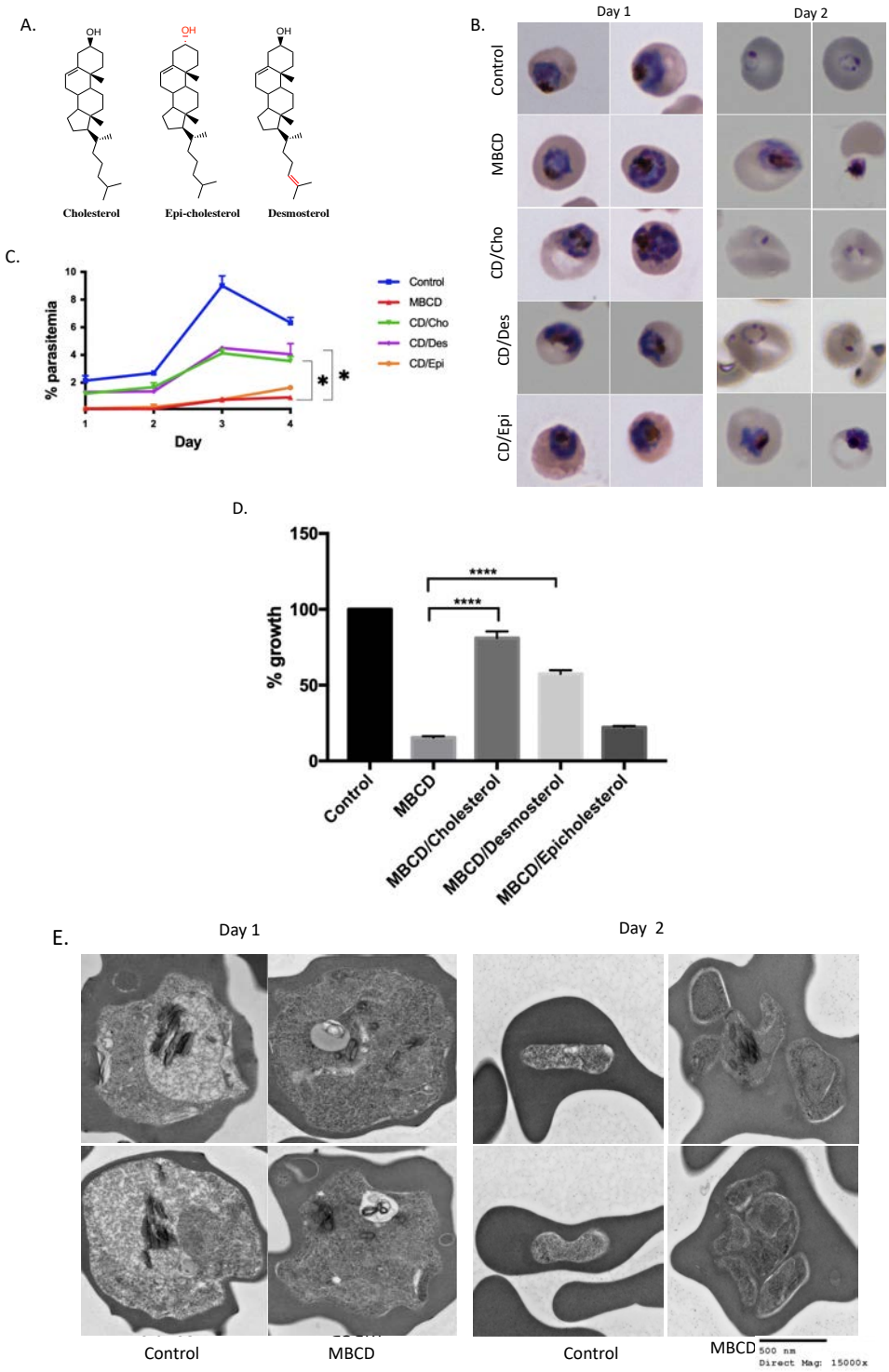

Figure 4: Cholesterol in the erythrocyte membrane is essential for growth and proliferation of *P. falciparum*.(A) Structure of MßCD, Cholesterol, Epicholesterol and Desmosterol. The differences between the structure of sterols are highlighted in red. (B) Giemsa-stained thin blood smears prepared from control, MßCD and erythrocytes reconstituted with cholesterol, desmosterol or epicholesterol at 24 and 48 hours after treatment. C) Parasitemia in 1:10 split

682 of ring stage parasites from control, MßCD (CD) or erythrocytes reconstituted with cholesterol
683 (CD/Cho), desmosterol(CD/Des) or epicholesterol (CD/Epi) over 4 days (~3000 cells were
684 counted). Based on one tailed unpaired *t-test* (* $p<0.05$). (D) Relative (^{3}H)-hypoxanthine
685 incorporation by ring stage parasites over a 24 hour period following treatment with MßCD or
686 reconstituted with cholesterol, desmosterol and epicholesterol. Based on unpaired t-test with
687 Welch's correction (* $p<0.05$, *** $p<0.001$). Error bars=mean±SD N=8. (E) TEM of the ring
688 stage erythrocyte treated with 5mM MßCD and imaged after 24 or 48 hours. (Left)After 24
689 hours, in erythrocyte treated with MßCD, parasites are unable to form normal trophozoites. The
690 nuclear membrane is indistinct, hemozoin is dispersed (indicated by arrows) and food vacuole
691 is small compared to control erythrocytes. (Right) After 48 hours, parasites in the control
692 culture were able to invade the erythrocyte and form rings while the parasites in the MßCD
693 treated erythrocytes undergo did not progress further and appear to disintegrate (Scale bar-
694 500nM, Direct magnification-15,000x).
695
696
697
698
699
700
701
702
703
704
705

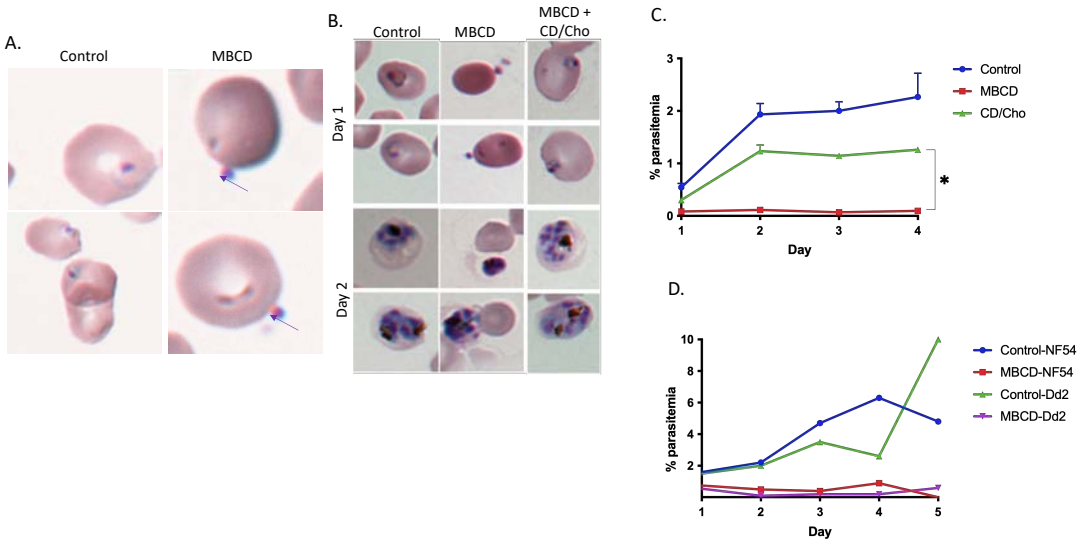

Figure 5: Reducing the cholesterol content in the erythrocyte membrane inhibits *P. falciparum* invasion

(A) Giemsa stained thin blood smears from control and MßCD treated erythrocytes after 24 hours. While ring stages were seen in the control erythrocytes, no invasion was seen in the MßCD treated erythrocytes but merozoites appeared to remain attached to the surface as indicated by arrows. (B) Percoll enriched trophozoites were added to erythrocytes treated with MßCD or reconstituted with cholesterol and giemsa stained thin blood smears were prepared at 24 and 48 hours. Reconstituted erythrocytes were able to support parasite growth. (C) Parasitemia from 1:10 split of culture from MßCD treated and reconstituted with cholesterol in normal erythrocytes over a period of 4 days (~3000 cells were counted). Based on Mann-Whitney test (* $p<0.05$) (D) Percoll synchronized trophozoites from NF54 and Dd2 strains were added onto MßCD treated erythrocytes. Parasitemia from 1:10 split of these cultures by examining Giemsa-stained thin blood smears (~1000 cells were counted).

Supplementary Figure Legends

Supplementary Figure 1: Images of extruded parasites following MßCD treatment of of the NF54 RhopH2/Exp2 transgenic line.

723 Representative images (out of >50) of live NF54 RhopH2/Exp2 line after MßCD treatment.
724 Erythrocyte membrane is stained with WGA-Alexa-350 (Blue), EXP2 is red and RhoH2 is
725 green. Infected erythrocytes were subjected to live fluorescent microscopy after treatment with
726 MßCD. Scale bar is 2 µm.

727 **Supplementary figure 2:** Phase contrast images of late stage *P. falciparum* extruded after
728 treatment with MßCD.
729 Infected erythrocytes were subjected to phase contrast microscopy after treatment with
730 MßCD. Extruded parasites are indicated by red arrows.

731 **Supplementary figure 3:** Phalloidin staining of MßCD treated cultures from PfVP1-NG
732 transgenic line: (A) Representative images of uninfected and infected cells from untreated
733 cultures after staining with Phalloidin AlexaFluor 594. (B) Representative images of
734 uninfected and infected cells from MßCD treated cultures followed by staining with
735 Phalloidin AlexaFluor 594. (Scale bar- 5 µm). Overall, 60-70% of uninfected as well as
736 infected erythrocyte cytoskeletons were stained with phalloidin, indicating membrane breach
737 without the lysis of erythrocytes.

738 **Supplementary figure 4:** Transmission electron microscopy of the ring stage erythrocyte
739 treated with 5mM MßCD and imaged after 24 (Day 1) or 48 hours (Day2)
740 (A) After 24 hours, the trophozoite like parasites in the MßCD treated cultures (lower panel)
741 have indistinct membranes, compromised food vacuole and dispersed hemozoin compared to
742 the controls (Upper panel) (B) After 48 hours, in the control culture (Upper panel) the
743 parasites invaded and formed rings while the parasites in the MßCD treated cultures (Lower
744 panel) failed to form mature merozoites (Scale bar-500nM, Direct magnification-15,000x).
745

746 **Supplementary Videos Legends**

747 **Supplementary video 1:** Treatment with MßCD causes extrusion of trophozoites from
748 erythrocytes
749 Representative time lapse video microscopy of the NF54 RhopH2/Exp2 line after MßCD
750 treatment. Erythrocyte membrane is stained with WGA-Alexa-350 (Blue). Infected
751 erythrocytes were subjected to live fluorescent microscopy after treatment with MßCD.
752 Parasites extrude out from erythrocyte without causing lysis of the erythrocyte. Video was
753 acquired using the Nikon Ti microscope. The interval between each frame was 4 sec and the
754 video was captured for a total 20 min (93 frames, FPS:0.09, frames 59-64 shown in the
755 video). Images were deconvoluted by Richardson Lucy algorithm using the Nikon NIS
756 elements software package and converted to .avi files.
757
758 **Supplementary video 2:** Cyt-D treatment does not inhibit MßCD mediated parasite
759 extrusion
760 Representative time lapse video microscopy of the NF54 RhopH2/Exp2 line after MßCD
761 treatment. Erythrocyte membrane is stained with WGA-Alexa-350 (Blue). Infected
762 erythrocytes were subjected to live fluorescent microscopy after treatment with Cyt-D
763 followed by treatment with MßCD. Treatment with Cyt-D does not inhibit MßCD mediated
764 extrusion of the parasite. Video microscopy was performed as mentioned above for video 1.
765 The interval between each frame was 31 sec and the video was captured for a total 5 min (11
766 frames, FPS:0.04, all 11 frames shown in the video)
767
768 **Supplementary movie 3:** Treatment with MßCD does not cause extrusion of ring stage
769 parasites
770 Erythrocytes infected with ring stages of the NF54 RhopH2/Exp2 were treated with MßCD .
771 Erythrocyte membrane is stained with WGA-Alexa-350 (Blue). Ring stage parasites do not

extrude out after MßCD treatment. Video microscopy was performed as mentioned for video 1. The interval between each frame was 31 secs and the video was captured for a total 5 mins (11 frames, FPS:0.04, all 11 frames shown in the video)

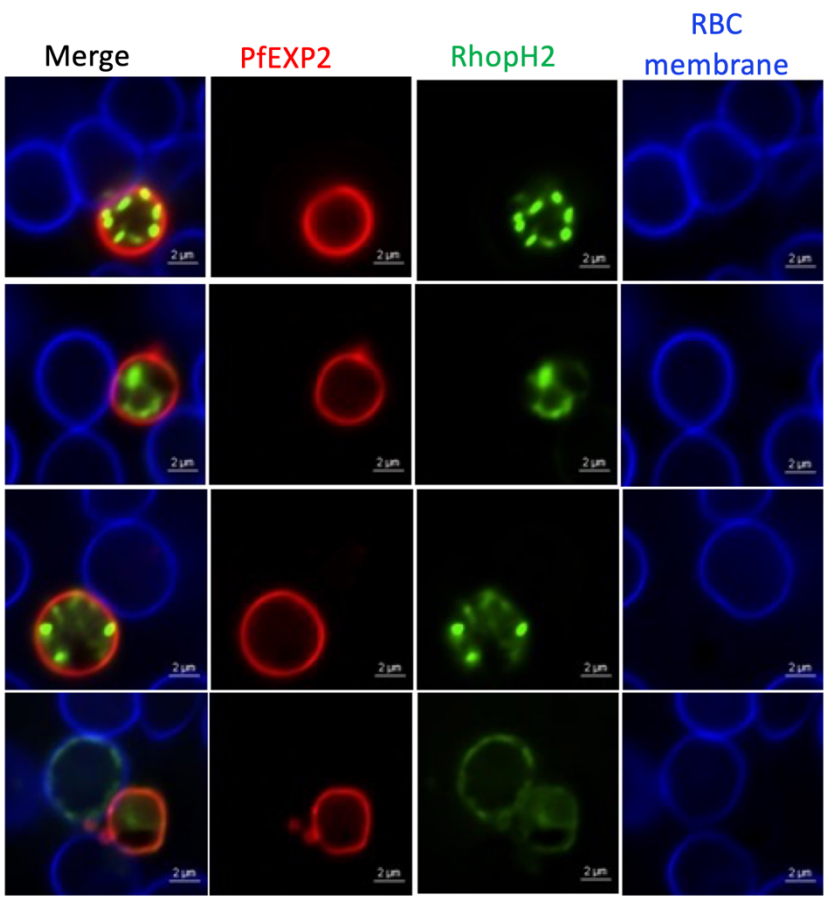

Supplementary Figure 1: Images of extruded parasites following MßCD treatment of of the NF54 RhopH2/Exp2 transgenic line.

Representative images (out of >50) of live NF54 RhopH2/Exp2 line after MßCD treatment. Erythrocyte membrane is stained with WGA-Alexa-350 (Blue), EXP2 is red and RhoH2 is green. Infected erythrocytes were subjected to live fluorescent microscopy after treatment with MßCD. Scale bar is 2 µm.

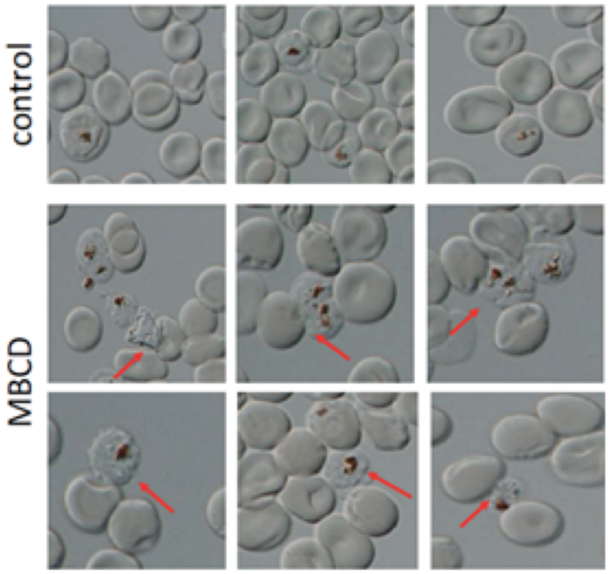

Supplementary figure 2: Phase contrast images of late stage *P. falciparum* extruded after treatment with MßCD.

Infected erythrocytes were subjected to phase contrast microscopy after treatment with MßCD. Extruded parasites are indicated by red arrows.

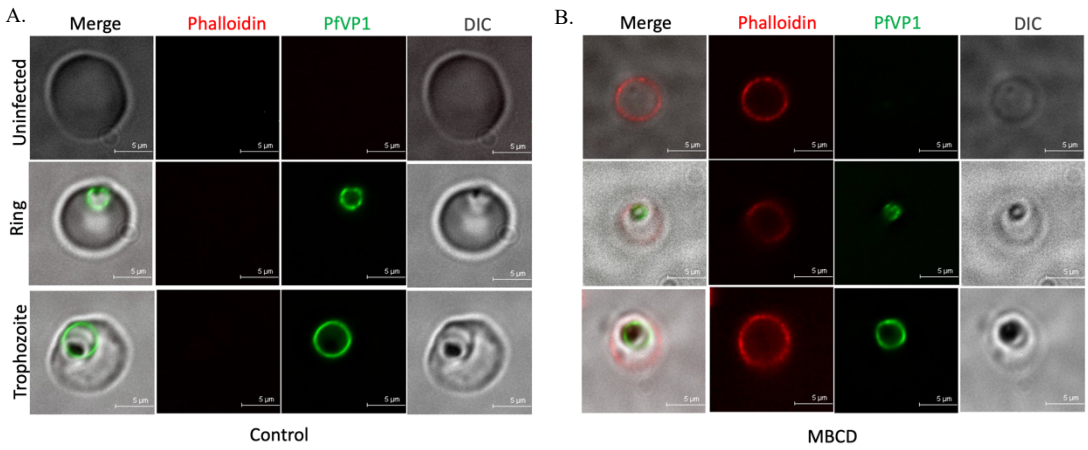

Supplementary figure 3: Phalloidin staining of MßCD treated cultures from PfVP1-NG transgenic line: (A) Representative images of uninfected and infected cells from untreated cultures after staining with Phalloidin AlexaFluor 594. (B) Representative images of uninfected and infected cells from MßCD treated cultures followed by staining with Phalloidin AlexaFluor 594. (Scale bar- 5 µm). Overall, 60-70% of uninfected as well as infected erythrocyte cytoskeletons were stained with phalloidin, indicating membrane breach without the lysis of erythrocytes.

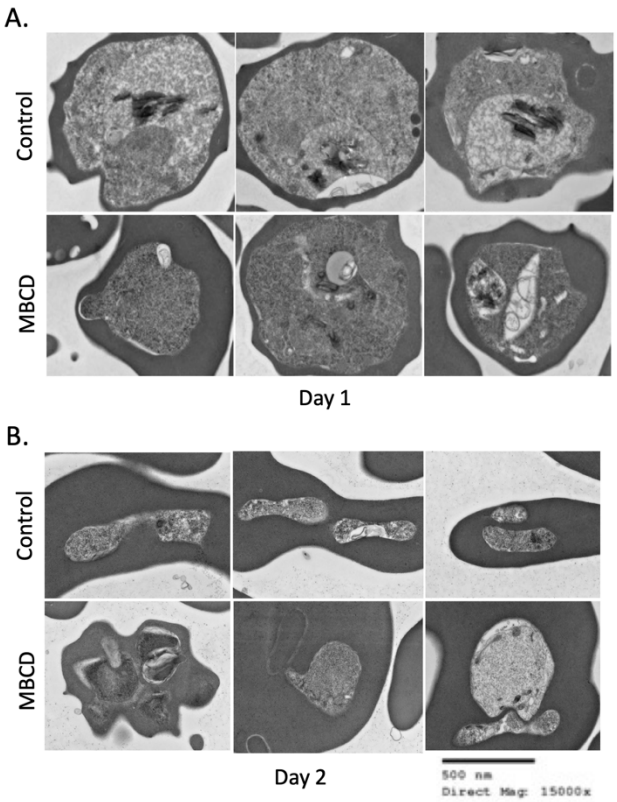

Supplementary figure 4: Transmission electron microscopy of the ring stage erythrocyte treated with 5mM MßCD and imaged after 24 (Day 1) or 48 hours (Day2)
(A) After 24 hours, the trophozoite like parasites in the MßCD treated cultures (lower panel) have indistinct membranes, compromised food vacuole and dispersed hemozoin compared to the controls (Upper panel) (B) After 48 hours, in the control culture (Upper panel) the parasites invaded and formed rings while the parasites in the MßCD treated cultures (Lower panel) failed to form mature merozoites (Scale bar-500nM, Direct magnification-15,000x).